Probing pair correlations in Fermi gases with Ramsey-Bragg interferometry

Théo Malas-Danzé,[1,2] Alexandre Dugelay,[1,2] Nir Navon,[2,3] and Hadrien Kurkjian[4]

[1]*ENS Paris-Saclay 91190 Gif-Sur-Yvette, France*
[2]*Department of Physics, Yale University, New Haven, Connecticut 06520, USA*
[3]*Yale Quantum Institute, Yale University, New Haven, Connecticut 06520, USA*
[4]*Laboratoire de Physique Théorique, Université de Toulouse, CNRS, UPS, 31400, Toulouse, France*
(Dated: December 19, 2023)

We propose an interferometric method to probe pair correlations in a gas of spin-1/2 fermions. The method consists of a Ramsey sequence where both spin states of the Fermi gas are set in a superposition of a state at rest and a state with a large recoil velocity. The two-body density matrix is extracted via the fluctuations of the transferred fraction to the recoiled state. In the pair-condensed phase, the off-diagonal long-range order is directly reflected in the asymptotic behavior of the interferometric signal for long interrogation times. The method also allows to probe the spatial structure of the condensed pairs: the interferometric signal is an oscillating function of the interrogation time in the Bardeen-Cooper-Schrieffer regime; it becomes an overdamped function in the molecular Bose-Einstein condensate regime.

Introduction: At low temperatures, the behavior of quantum matter is often marked by the emergence of coherent ordered phases displaying remarkable macroscopic properties. Such condensed phases appear in various contexts, such as solid-state physics [1], nuclear or neutron matter [2], and ultracold atomic gases [3, 4]. They are characterized by long-range coherence carried by a macroscopically occupied wavefunction. In the simple case of the weakly interacting Bose gas, this order shows up as off-diagonal long-range order (ODLRO) in the one-body density matrix $\rho_1(\mathbf{r}, \mathbf{r}') = \langle \hat{\Psi}^\dagger(\mathbf{r})\hat{\Psi}(\mathbf{r}')\rangle$ (where $\hat{\Psi}$ is the Bose field operator), such that $\lim_{|\mathbf{r}-\mathbf{r}'|\to\infty} \rho_1(\mathbf{r}, \mathbf{r}') = n_0$ is the density of the Bose-Einstein condensate (BEC). The ODLRO in a Bose gas has been measured for instance via the single-particle momentum distribution [5, 6], which for a translationally invariant system, is the Fourier transform of ρ_1.

In spin-1/2 Fermi systems, the one-body density matrix cannot exhibit ODLRO, owing to Pauli's exclusion principle, and the momentum distribution remains smooth across the phase transition [7]. Instead, a macroscopically occupied wavefunction characteristic of the pair condensate can only appear in the pair density matrix $\rho_2(\mathbf{r}_1, \mathbf{r}_2, \mathbf{r}'_1, \mathbf{r}'_2) = \langle \hat{\Psi}^\dagger_\uparrow(\mathbf{r}_1)\hat{\Psi}^\dagger_\downarrow(\mathbf{r}_2)\hat{\Psi}_\downarrow(\mathbf{r}'_2)\hat{\Psi}_\uparrow(\mathbf{r}'_1)\rangle$ (where $\hat{\Psi}_\sigma$ is the Fermi field operator for the fermion of spin σ) [3, 8]. Measurements of ODLRO are for this reason considerably more challenging in Fermi systems. Rapid ramps of the magnetic field have been used to project the pair condensate onto a BEC of molecules [9–12]; however, the measured molecular fraction is notoriously difficult to interpret theoretically, owing to the various two- and many-body time scales involved in the problem [13]. Measurement of pair correlations in time-of-flight images have been proposed as a way to access ODLRO [14, 15]; an analogous protocol has been implemented, albeit on a small Fermi system [16].

Interferometric protocols offer an alternative route to measure the coherence properties of quantum gases. Cold-atom experiments are particularly well-suited for matter-wave interferometry, thanks to the possibilities of creating a coherent copy of the gas by manipulating the internal or external state of the atoms [17]. In Bose gases, direct real-space measurements of $\rho_1(\mathbf{r}, \mathbf{r}')$ were performed using Ramsey protocols relying on interferometry of Bragg-diffracted gases [18–20] In Fermi gases, matter-wave interference between small atom numbers extracted by spatially-resolved Bragg pulses were proposed as a way to measure ρ_2 [21].

Inspired by such techniques, we propose a protocol to measure ρ_2 from the fluctuations of a Ramsey-Bragg interferometer. A copy of the spin-1/2 Fermi gas is created by imparting a large velocity to a fraction of the atoms. Interactions are turned off and the copy travels ballistically, thereby stretching or translating the pairs of fermions by a distance proportional to the interrogation time. When the interferometric sequence is closed by the second pulse, the stretched and translated pairs interfere with those at rest, and a measurement of the correlation between the number of spin ↑ and spin ↓ recoiling atoms reveals the most important features of ρ_2. In the pair-condensed phase, the interferometric signal carries information on the magnitude of the fermionic condensate and on the wavefunction of the fermionic pairs.

Interferometric protocol: In Fig. 1 we show a sketch of the proposed measurement protocol. We consider a homogeneous spin-1/2 Fermi gas in a cubic box of size L [22]. At $t = 0$, a first Bragg pulse is shined on the gas for a duration t_{pulse}. We place ourselves in the regime of a short and intense pulse, designed to be resonant with the whole gas and to create a moving copy of the cloud whose momentum distribution does not overlap with the original one (see Fig. 1). Both spin states are in a superposition of two components: a copy with no average momentum, and a copy with a large average momentum $\mathbf{q}_\text{r}$. Assuming that the gas initially has zero mean velocity, the energy transferred by the pulse is adjusted to $\hbar\omega = \epsilon_{\mathbf{q}_\text{r}}$ (where $\epsilon_\mathbf{k} = \hbar^2 k^2/2m$ is the kinetic energy and m is the mass of the fermion), in resonance with the atoms at rest. Since the atoms travelling at a velocity $\hbar\mathbf{k}/m \neq \mathbf{0}$ experience a detuning $\hbar\omega - \epsilon_{\mathbf{k}+\mathbf{q}_\text{r}} + \epsilon_\mathbf{k} = -\hbar^2\mathbf{q}_\text{r} \cdot \mathbf{k}/m$, the duration of the pulse t_{pulse} should be short enough so that this detuning remains negligible over the typical range δk of the momentum

distribution of the gas:

$$\frac{\hbar^2 q_{\rm r} \delta k}{m} t_{\rm pulse} \ll 1. \tag{1}$$

To evaluate this condition, let us consider the case of contact interactions between $\uparrow$ and $\downarrow$ fermions, characterized by a s-wave scattering length a. On the Bardeen-Cooper-Schrieffer side (BCS, $a < 0$), one can estimate $\delta k \approx \rho^{1/3}$, where ρ is the total density and on the molecular Bose-Einstein condensate side (BEC, $a > 0$) $\delta k \approx 1/a$. In this limit, the broadening of the momentum distribution implies that fulfilling both inequalities for $t_{\rm pulse}$ will no longer be possible at fixed $q_{\rm r}$. Note that the pulse duration should also be long enough $(\hbar^2 q_{\rm r}^2/m) t_{\rm pulse} \gg 1$ such that second-order transitions to states of momenta $\mathbf{k} + 2\mathbf{q}_{\rm r}$ or $\mathbf{k} - \mathbf{q}_{\rm r}$ remain negligible.

In this intense-pulse regime, the gas can be approximated by a two-level system undergoing Rabi oscillations between a state *at rest* (violet distribution in the upper sketches of Fig. 1) and a *recoiling* one (green distribution). The evolution during the first Bragg pulse corresponds to a rotation of angle $\theta = \Omega_{\rm R} t_{\rm pulse}$ (where $\Omega_{\rm R}$ is the Rabi frequency of the Bragg pulse) on the Bloch sphere of this effective two-level system:

$$\begin{pmatrix} \hat{a}_{\mathbf{k},\sigma} \\ \hat{a}_{\mathbf{k}+\mathbf{q}_{\rm r},\sigma} \end{pmatrix}(t_{\rm pulse}) = \mathscr{S}(\theta,0)\begin{pmatrix} \hat{a}_{\mathbf{k},\sigma} \\ \hat{a}_{\mathbf{k}+\mathbf{q}_{\rm r},\sigma} \end{pmatrix}(0). \tag{2}$$

Here $\hat{a}_{\mathbf{k},\sigma}$ annihilates a fermion of wavevector $\mathbf{k}$ and spin σ and the matrix $\mathscr{S}(\theta,\phi) = \begin{pmatrix} \cos(\theta/2) & -i\sin(\theta/2)e^{i\phi} \\ -i\sin(\theta/2)e^{-i\phi} & \cos(\theta/2) \end{pmatrix}$ describes a rotation of angle θ around the vector $(\cos\phi, -\sin\phi, 0)$ of the equatorial plane of the Bloch sphere.

After this first pulse, the recoiling and non-recoiling components evolve ballistically during an interrogation time τ. By contrast to the Ramsey-Bragg interferometry of weakly interacting gases [18, 19], it is crucial that interactions are turned off in strongly interacting gases before the first Bragg pulse. This would mitigate both fast many-body evolution during the interrogation sequence, and the high collisional density that would prevent the diffracted component to fly freely [23].

This could be achieved either with a fast Feshbach field ramp or with fast Raman pulses [16, 24]. The recoiling component travels a distance $\mathbf{x}_\tau \equiv \hbar\tau \mathbf{q}_{\rm r}/m$, at a velocity sufficiently large to exit the trapping potential (in the direction of propagation). This means that only a fraction $(1 - x_\tau/L)$ of the cloud remains within the box volume after the interrogation time (assuming $\mathbf{q}_{\rm r}$ is aligned with an axis of the cubic trap) and gives an upper limit $\tau < mL/\hbar q_{\rm r}$ to the interrogation time.

After the interrogation time, the dephasing between the recoiling and non-recoiling components is $\varphi_{\mathbf{k}}(\tau) = ((\epsilon_{\mathbf{k}+\mathbf{q}_{\rm r}} - \epsilon_{\mathbf{k}})/\hbar - \omega)\tau$ relatively to the Bragg transition, and a second Bragg pulse recombines the two components:

$$\begin{pmatrix} \hat{a}_{\mathbf{k},\sigma} \\ \hat{a}_{\mathbf{k}+\mathbf{q}_{\rm r},\sigma} \end{pmatrix}(\tau + 2t_{\rm pulse}) = \mathscr{S}(\theta,\omega\tau)\begin{pmatrix} \hat{a}_{\mathbf{k},\sigma} \\ \hat{a}_{\mathbf{k}+\mathbf{q}_{\rm r},\sigma} \end{pmatrix}(\tau + t_{\rm pulse}) \tag{3}$$

$$= \mathscr{S}(\theta,\varphi_{\mathbf{k}}(\tau))\mathscr{S}(\theta,0)\begin{pmatrix} \hat{a}_{\mathbf{k}} \\ \hat{a}_{\mathbf{k}+\mathbf{q}_{\rm r}} \end{pmatrix}(0).$$

Eq. (3) thus describes a Ramsey sequence with a dephasing $\varphi_{\mathbf{k}}(\tau)$ that depends on the initial momentum of the atoms[1]. This makes the interferometer sensitive to the spatial structure of the gas, where short interrogation times allow to probe short-range correlations, and long times probing long-range correlations.

At the end of the interferometric sequence, the recoiling atoms are a superposition of atoms initially present in different positions of the gas:

$$\hat{\Psi}_{{\rm r},\sigma}(\mathbf{r}) = -i\frac{\sin\theta}{2}\left(\hat{\Psi}_\sigma(\mathbf{r}) + \hat{\Psi}_\sigma(\mathbf{r} - \mathbf{x}_\tau)\right), \tag{4}$$

where $\hat{\Psi}_\sigma(\mathbf{r})$ is the field operator at $t = 0$ and $\hat{\Psi}_{r,\sigma} = (1/\sqrt{L^3})\sum_{\mathbf{k}\in\mathcal{B}} e^{i(\epsilon_{\mathbf{k}}\tau - \mathbf{k}\cdot\mathbf{r})}\hat{a}_{\mathbf{k},\sigma}(\tau)$ is the field operator of recoiling atoms at $t = \tau$ (the free evolution during the interrogation time is treated in the interaction representation); the summation over $\mathbf{k}$ includes here only the recoiling atoms (*i.e.* $\mathcal{B}$ is a neighborhood around $\mathbf{q}_{\rm r}$ of typical size δk, small compared to $q_{\rm r}$). For pairs of $\uparrow$ and $\downarrow$ atoms, this yields the superposition depicted in Fig. 1:

$$\hat{\Psi}_{{\rm r},\downarrow}(\mathbf{r}_2)\hat{\Psi}_{{\rm r},\uparrow}(\mathbf{r}_1) = -\frac{\sin^2\theta}{4}\left[\hat{\Psi}_\downarrow(\mathbf{r}_2)\hat{\Psi}_\uparrow(\mathbf{r}_1) + \hat{\Psi}_\downarrow(\mathbf{r}_2)\hat{\Psi}_\uparrow(\mathbf{r}_1 - \mathbf{x}_\tau) + \hat{\Psi}_\downarrow(\mathbf{r}_2 - \mathbf{x}_\tau)\hat{\Psi}_\uparrow(\mathbf{r}_1) + \hat{\Psi}_\downarrow(\mathbf{r}_2 - \mathbf{x}_\tau)\hat{\Psi}_\uparrow(\mathbf{r}_1 - \mathbf{x}_\tau)\right]. \tag{5}$$

The four terms represent respectively a pair at rest, a pair where the $\uparrow$ or the $\downarrow$ fermion has been stretched by $\mathbf{x}_\tau$, and a pair globally translated by $\mathbf{x}_\tau$.

After the Ramsey sequence is closed, the recoiling atoms are spatially separated from the atoms at rest by a time of flight $t_{\rm tof}$. An absorption image is then taken for each spin

---

[1] Note that the dephasing $\varphi_{\mathbf{k}}(2t_{\rm pulse})$ accumulated during the two Bragg pulses is negligible by virtue of Eq. (1).
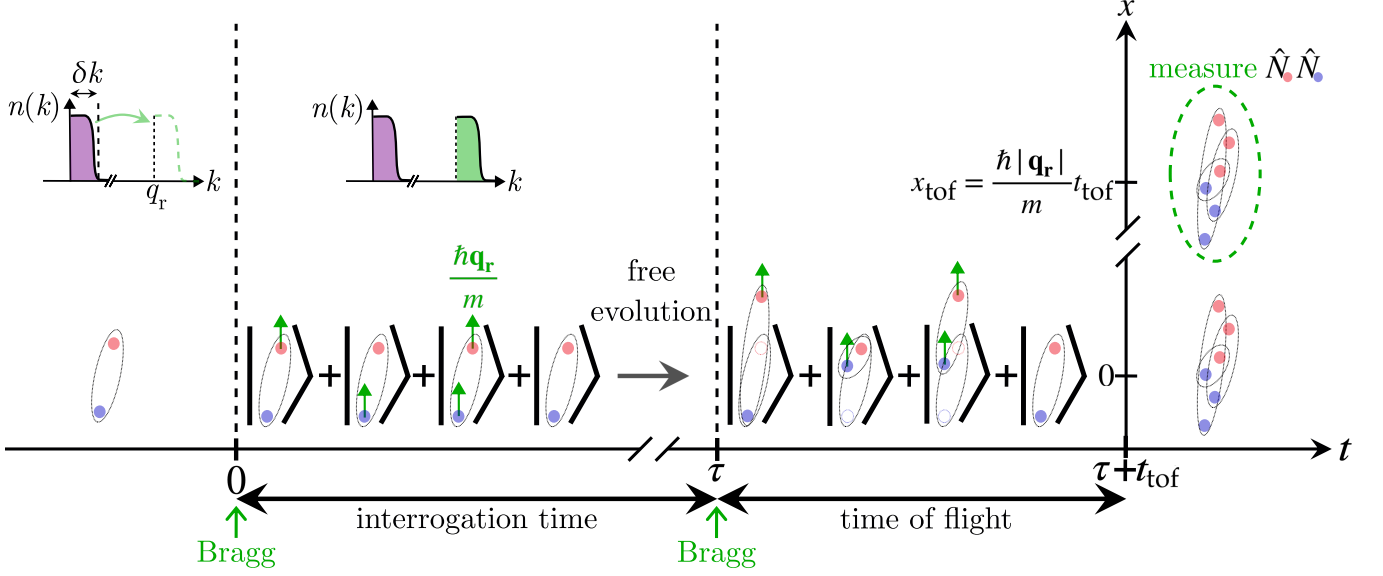
FIG. 1. (a) Sketch of the Ramsey-Bragg interferometer applied to a pair of fermions. The blue (resp. red) circles represent spin $\uparrow$ (resp. $\downarrow$) atoms. The Bragg pulses create superpositions of atoms at rest and moving with a recoil momentum $q_{\rm r}$. After the time of flight, the component at rest and the recoiling one are separated by $x_{\rm tof}$. For clarity, the finite pulse duration $t_{\rm pulse}$ is not shown.

to measure the number $\hat{N}_{{\rm r},\sigma}$ of recoiling atoms of spin σ:

$$\hat{N}_{{\rm r},\sigma} \equiv \int \hat{\Psi}_{{\rm r},\sigma}^{\dagger}(\mathbf{r})\hat{\Psi}_{{\rm r},\sigma}(\mathbf{r})\mathrm{d}\mathbf{r} \quad (6)$$

$$= \frac{\sin^2\theta}{2}\left[\hat{N}_{\sigma} + \hat{\rho}_{1,\sigma}(\mathbf{x}_{\tau})\right]. \quad (7)$$

Here, $\hat{N}_{\sigma}$ is the total number of atoms of spin σ, and $\hat{\rho}_{1,\sigma}(\mathbf{x}_{\tau}) = \int \hat{\Psi}_{\sigma}^{\dagger}(\mathbf{r})\hat{\Psi}_{\sigma}(\mathbf{r} - \mathbf{x}_{\tau})\mathrm{d}\mathbf{r}$ is the one-body correlation operator. We assumed that $\hat{\rho}_{1,\sigma}$ is parity symmetric, *i.e.* $\hat{\rho}_{1,\sigma}(-\mathbf{x}_{\tau}) = \hat{\rho}_{1,\sigma}(\mathbf{x}_{\tau})$.

Measuring long-range pair ordering: To measure ρ_2, we propose to record the correlations between the numbers of recoiling atoms of spin $\uparrow$ and $\downarrow$:

$$S(\mathbf{x}_{\tau}) = \langle\hat{N}_{{\rm r},\uparrow}(\mathbf{x}_{\tau})\hat{N}_{{\rm r},\downarrow}(\mathbf{x}_{\tau})\rangle - \langle\hat{N}_{{\rm r},\uparrow}(\mathbf{x}_{\tau})\rangle\langle\hat{N}_{{\rm r},\downarrow}(\mathbf{x}_{\tau})\rangle. \quad (8)$$

This interferometric signal is constructed by statistically averaging individual realizations of $N_{{\rm r},\uparrow}$ and $N_{{\rm r},\downarrow}$. It contains the following contractions of ρ_2:

$$f_{\rm tr}(\mathbf{x}_{\tau}) = \int \rho_2(\mathbf{r}_1 - \mathbf{x}_{\tau}, \mathbf{r}_2 - \mathbf{x}_{\tau}; \mathbf{r}_1, \mathbf{r}_2)\mathrm{d}\mathbf{r}_1\mathrm{d}\mathbf{r}_2 \quad (9)$$

$$f_{{\rm str},\uparrow}(\mathbf{x}_{\tau}) = \int \rho_2(\mathbf{r}_1 - \mathbf{x}_{\tau}, \mathbf{r}_2; \mathbf{r}_1, \mathbf{r}_2)\mathrm{d}\mathbf{r}_1\mathrm{d}\mathbf{r}_2 \quad (10)$$

$$f_{{\rm str},\downarrow}(\mathbf{x}_{\tau}) = \int \rho_2(\mathbf{r}_1, \mathbf{r}_2 - \mathbf{x}_{\tau}; \mathbf{r}_1, \mathbf{r}_2)\mathrm{d}\mathbf{r}_1\mathrm{d}\mathbf{r}_2 \quad (11)$$

$$f_{{\rm str},\uparrow\downarrow}(\mathbf{x}_{\tau}) = \int \rho_2(\mathbf{r}_1 - \mathbf{x}_{\tau}, \mathbf{r}_2; \mathbf{r}_1, \mathbf{r}_2 - \mathbf{x}_{\tau})\mathrm{d}\mathbf{r}_1\mathrm{d}\mathbf{r}_2. \quad (12)$$

These functions have a simple interpretation: $f_{\rm tr}$ measures the overlap between the translated and the original pair of Eq. (5),

$f_{{\rm str},\sigma}$ the overlap between the pair stretched by the spin σ fermion and the original one, and $f_{{\rm str},\uparrow\downarrow}$ the overlap between the two pairs stretched by the opposite spin fermion. Using Eq. (7), we find:

$$S = \frac{\sin^4\theta}{4}\left[f_{{\rm str},\uparrow} + f_{{\rm str},\downarrow} + \frac{f_{{\rm str},\uparrow\downarrow} + f_{\rm tr}}{2} \right.$$
$$\left. -\rho_{1,\uparrow}\rho_{1,\downarrow} - N_{\uparrow}\rho_{1,\downarrow} - N_{\downarrow}\rho_{1,\uparrow}\right], \quad (13)$$

where $\rho_{1,\sigma} \equiv \langle\hat{\rho}_{1,\sigma}(\mathbf{x}_{\tau})\rangle$. The signal S is maximum for $\theta = \pi/2$; we set θ to this value from now on. When the gas is in the normal phase, all the functions $f_{\rm str}$, $f_{\rm tr}$ and ρ_1 vanish at large distances. On the contrary, when the gas is pair condensed, the contribution of translated pairs $f_{\rm tr}$ does not vanish when $x_{\tau} \to +\infty$. In this case, ρ_2 has a macroscopic eigenvalue N_0 associated to a wavefunction ϕ_0 and behaves at large distances (that is, when the pair center of mass $\mathbf{R} = |\mathbf{r}_1 + \mathbf{r}_2|/2$ and $\mathbf{R}' = |\mathbf{r}_1' + \mathbf{r}_2'|/2$ are infinitely separated) as

$$\lim_{|\mathbf{R}-\mathbf{R}'|\to+\infty} \rho_2(\mathbf{r}_1, \mathbf{r}_2, \mathbf{r}_1', \mathbf{r}_2') = N_0\phi_0^*(\mathbf{r}_1, \mathbf{r}_2)\phi_0(\mathbf{r}_1', \mathbf{r}_2'), \quad (14)$$

This implies that $\lim_{x_{\tau}\to+\infty} f_{\rm tr}(\mathbf{x}_{\tau}) = N_0$, such that

$$S_{\infty} \equiv \lim_{x_{\tau}\to+\infty} S(\mathbf{x}_{\tau}) = \frac{N_0}{8}. \quad (15)$$

We have assumed here that possible fluctuations of the atom numbers are uncorrelated ($\langle\hat{N}_{\uparrow}\hat{N}_{\downarrow}\rangle = N_{\uparrow}N_{\downarrow}$). Eq. (15) provides a direct measurement of the magnitude of the long-range order N_0, a quantity that cannot be measured by the rapid-ramp technique [9, 10]. Note that N_0 cannot be interpreted as
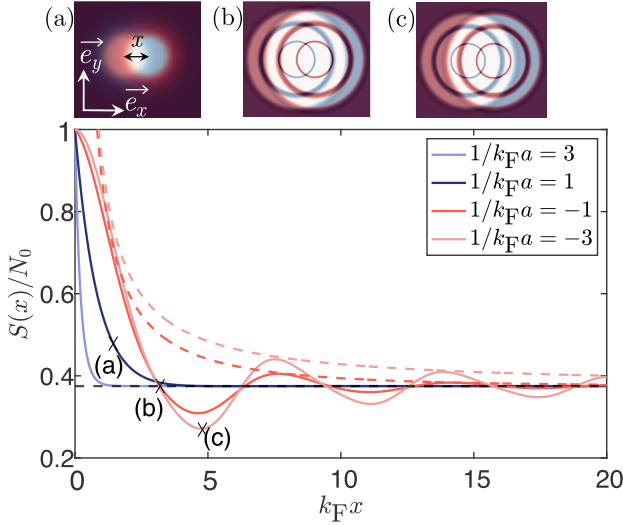
FIG. 2. The interferometric signal $S(x)$ as a function of the distance $x = x_{\tau,\uparrow} = x_{\tau,\downarrow}$ for different values of the interaction strength, calculated using the mean-field BCS theory (solid curves). On the BCS side, where S oscillates, the envelope is $(x_0/\pi x)\exp(-x/\xi_x)$[211] (dashed lines). (a)-(c) Sketches of the interference patterns for S originating from the condensate wavefunction ϕ_0. The copy at[212] rest is shown in blue ($|\phi_0(\mathbf{r}_1,\mathbf{r}_2)|^2$) and the translated one in red ($|\phi_0(\mathbf{r}_1,\mathbf{r}_2+\mathbf{x}_\tau)|^2$), where $x = |\mathbf{x}_\tau|$; (a) in the BEC regime, (b) in[213] the BCS regime, where the displacement x corresponds to the first[214] cancellation of S (see main panel), and (c) in the BCS regime, where[215] the displacement corresponds to the first minimum of S.

[193] the number of condensed pairs away from the BEC limit[2].

[194]   The contribution of the stretched pairs to S through $f_{\mathrm{str},\sigma}$[218]
[195] and $f_{\mathrm{str},\uparrow\downarrow}$, although negligible at distances larger than the
[196] pair size ξ_{pair}, carries essential information on the condensate
[197] wavefunction ϕ_0. It is possible to isolate the contribution of[219]
[198] $f_{\mathrm{str},\sigma}$ using a spin-dependent Bragg pulse, such that the dis-[220]
[199] placements $\mathbf{x}_{\tau,\uparrow}$ and $\mathbf{x}_{\tau,\downarrow}$ of the two spins no longer coincide.[221]
[200] For $\mathbf{x}_{\tau,\downarrow} = \mathbf{0}$ and $\mathbf{x}_{\tau,\uparrow} \neq \mathbf{0}$, Eq. (13) becomes[222]

[223]
[201]
$$S(\mathbf{x}_{\tau\uparrow}) = \frac{f_{\mathrm{str},\uparrow}(\mathbf{x}_{\tau\uparrow}) - N_\downarrow\rho_{1,\uparrow}(\mathbf{x}_{\tau\uparrow})}{2}. \quad (16)$$
[224]
[225]

[202] This result can be used to reveal the momentum structure of[226]
[203] ϕ_0. If the system is isotropic and translationally invariant,[227]
[204] and the pairs are tightly bound (as in the BEC limit), then
[205] $\phi_0(\mathbf{r}_1,\mathbf{r}_2)$ decreases rapidly and almost monotonically with[228]
[206] $x = |\mathbf{r}_1 - \mathbf{r}_2|$, and so does $f_{\mathrm{str},\sigma}$; the corresponding behav-
[207] ior for S is schematically depicted in Fig. 2(a). Conversely, if[229]
[208] pairing occurs at a nonzero wavenumber, as in the BCS limit,
[209] ϕ_0 oscillate with $|\mathbf{r}_1 - \mathbf{r}_2|$ at the corresponding wavelength
[210] and so does $f_{\mathrm{str},\sigma}$ (see Figs. 2(b)-(c)). [230]

---

[231]
[2] The condensate annihilation operator $\hat{b}_0$ =[232] $\int \phi_0^*(\mathbf{r}_1,\mathbf{r}_2)\hat{\Psi}_\downarrow(\mathbf{r}_1)\hat{\Psi}_\uparrow(\mathbf{r}_2)d\mathbf{r}_1 d\mathbf{r}_2$ is not bosonic, as $\left\langle\left[\hat{b}_0,\hat{b}_0^\dagger\right]\right\rangle \leq 1$ (the inequality is saturated only in the BEC limit). Therefore, $N_0 = \langle\hat{b}_0^\dagger\hat{b}_0\rangle$ is not the number of atoms in the condensate in the general case.

BCS mean-field approximation: To obtain a more explicit expression for S, and illustrate its behavior when $x_\tau \approx \xi_{\mathrm{pair}}$, we now use the BCS approximation and assume that the gas is balanced, such that $N_\uparrow = N_\downarrow$, $f_{\mathrm{str},\uparrow} = f_{\mathrm{str},\downarrow}$ and $\rho_{1,\uparrow} = \rho_{1,\downarrow}$. The total density $\rho = \rho_\uparrow + \rho_\downarrow$ defines the Fermi wavenumber $k_{\mathrm{F}} = (3\pi^2\rho)^{1/3}$, and in the BCS state ρ_2 factorizes into

$$\rho_2(\mathbf{r}_1,\mathbf{r}_2,\mathbf{r}_1',\mathbf{r}_2') = N_0\phi_0^*(\mathbf{r}_1,\mathbf{r}_2)\phi_0(\mathbf{r}_1',\mathbf{r}_2') \\ + \rho_1(\mathbf{r}_1,\mathbf{r}_1')\rho_1(\mathbf{r}_2,\mathbf{r}_2'). \quad (17)$$

Assuming that the gas is translationally invariant and isotropic, the functions previously defined in Eqs. (9)–(12) depend only on $x_\tau = |\mathbf{x}_\tau|$. Taking into account that the number is not fixed in the BCS state, $\langle\hat{N}_\uparrow\hat{N}_\downarrow\rangle \neq N_\uparrow N_\downarrow$,

$$S(x_\tau) = \frac{1}{8}\Bigg\{2\Big(\langle\hat{N}_\uparrow\hat{N}_\downarrow\rangle - N_\uparrow N_\downarrow\Big) \\ + N_0\Big[1 + 4f(x_\tau) + f(2x_\tau)\Big]\Bigg\}. \quad (18)$$

Here the function

$$f(x) = \int \phi_0^*(\mathbf{r}_1 - \mathbf{x},\mathbf{r}_2)\phi_0(\mathbf{r}_1,\mathbf{r}_2)d\mathbf{r}_1 d\mathbf{r}_2 \quad (19)$$

is the overlap between a stretch and an original pair of the condensate; it is related to the functions introduced before by $f_{\mathrm{str},\sigma} = N_0 f + N_\sigma\rho_1$ and $f_{\mathrm{str},\uparrow\downarrow}(x) = N_0 f(2x) + \rho_1^2(x)$. The condensate wavefunction in Fourier space $\phi_{\mathbf{k}}$, defined as $\phi_0(\mathbf{r}_1,\mathbf{r}_2) = \sum_{\mathbf{k}}\phi_{\mathbf{k}}e^{-i\mathbf{k}\cdot(\mathbf{r}_1-\mathbf{r}_2)}/L^3$, takes the form

$$\phi_{\mathbf{k}} = \frac{\Delta}{2E_{\mathbf{k}}\sqrt{N_0^{\mathrm{BCS}}}}, \quad (20)$$

where Δ is the gap, $E_{\mathbf{k}} = \sqrt{(\epsilon_{\mathbf{k}} - \mu)^2 + \Delta^2}$ is the BCS dispersion relation, and μ is the chemical potential. The associated macroscopic eigenvalue is $N_0^{\mathrm{BCS}} = \sum_{\mathbf{k}}\Delta^2/(4E_{\mathbf{k}}^2)$. The maximum of $|\phi_{\mathbf{k}}|$ is reached at the minimum of the BCS dispersion relation, that is, at $k_{\min} = \sqrt{2m\mu}/\hbar$ on the BCS side ($\mu > 0$) and $k = 0$ on the BEC side ($\mu < 0$). Using the BCS condensate wavefunction Eq. (20), we can perform the integral over $\mathbf{k}$ analytically in Eq. (19), which yields

$$f(x) = e^{-x/\xi_x}\mathrm{sinc}(\pi x/x_0), \quad (21)$$

where

$$\xi_x^2 = \frac{\hbar^2}{m\Delta}\left(\frac{\mu}{\Delta} + \sqrt{1 + \frac{\mu^2}{\Delta^2}}\right) \quad (22)$$

$$\frac{x_0^2}{\pi^2} = \frac{\hbar^2}{m\Delta}\frac{1}{\frac{\mu}{\Delta} + \sqrt{1 + \frac{\mu^2}{\Delta^2}}}. \quad (23)$$

Whether or not oscillations are visible before S reaches its asymptotic value[3] depends on the ratio x_0/ξ_x. In the BCS

---

[3] As seen in Fig. 2, BCS theory predicts that $\lim_{x_\tau \to \infty} S = S_\infty^{\mathrm{BCS}} =$
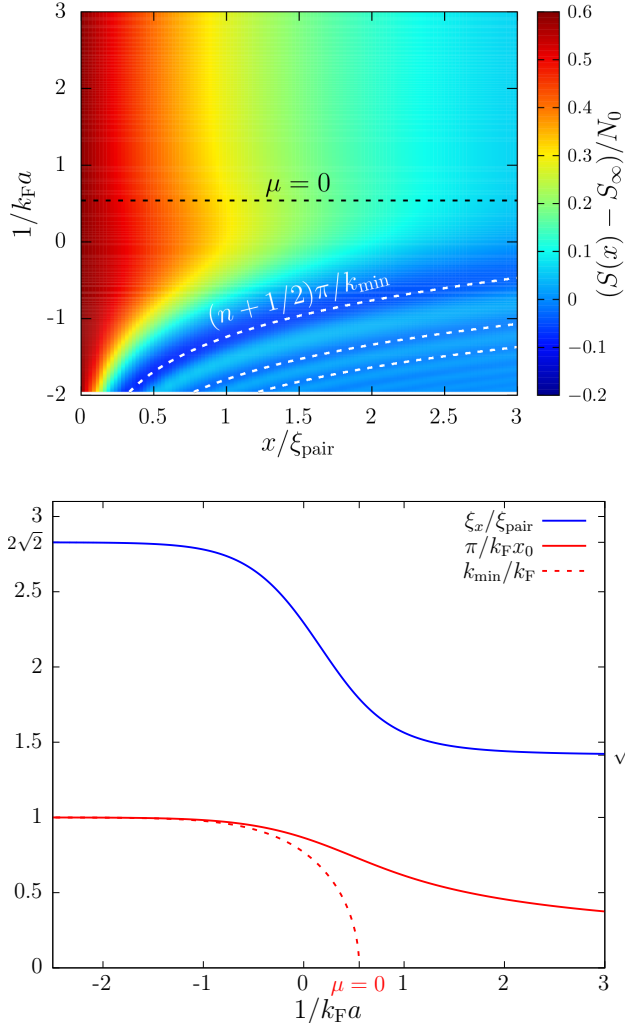
FIG. 3. (Top panel) The interferometric signal $S(x) - S_\infty$ normalized to N_0 as a function of $x/\xi_{\rm pair}$ and $1/k_{\rm F}a$ within the mean-field BCS approximation. The boundary between the BEC and BCS regime ($\mu = 0$ at $1/k_{\rm F}a \simeq 0.54$) is marked by the black dashed line. On the BCS side, we compare the local minima of the oscillatory signal to $x_n = (n+1/2)\pi/k_{\rm min}$ (white dashed curves). (Bottom panel) The wavenumber π/x_0 (normalized to $k_{\rm F}$) and the exponential attenuation length ξ_x (normalized to the Cooper pair size $\xi_{\rm pair}$) of the overlap function f in the BEC-BCS crossover. The dashed red curve shows the location of the dispersion minimum $k_{\rm min} = \sqrt{2m\mu}/\hbar$ on the BCS side ($\mu > 0$).

limit ($\mu/\Delta \to +\infty$ or $k_{\rm F}a \to 0^-$), the oscillation length $x_0 \sim \pi/k_{\rm F}$ is much shorter than the exponential-decay length $\xi_x \sim \hbar^2 k_{\rm F}/m\Delta$ which diverges as $O(\xi_{\rm pair})$. Thus, in the BCS regime, S exhibits oscillations (the dark and light red curves in Fig. 2 correspond to $1/k_{\rm F}a = -1$ and -3); the oscillations decay as a cardinal sine, on a typical length scale $1/k_{\rm F}$.

Conversely, in the BEC limit ($\mu/\Delta \to -\infty$ or $k_{\rm F}a \to 0^+$), $\xi_x \sim a$ tends to zero like the size of the bosonic dimers. At the same time, the oscillation frequency diverges as $x_0 \sim \sqrt{3\pi/4k_{\rm F}a}\,(\pi/k_{\rm F})$, such that no oscillations are visible in this regime (the dark and light blue curves on Fig. 2 correspond to $1/k_{\rm F}a = 1$ and 3). A transition between the two regimes (illustrated on the top panel of Fig. 3) occurs around the point where $\xi_x = x_0/\pi$, that is $\mu = 0$, which remarkably coincides with the point where the minimum $k_{\rm min}$ of the BCS dispersion relation reaches 0. We note that a measurement of the BCS gap is also accessible through the relation

$$\frac{\xi_x x_0}{\pi} = \frac{\hbar^2}{m\Delta}. \tag{24}$$

In Fig. 3, we compare ξ_x to the pair size defined as $\xi_{\rm pair} = (\int \rho_2(\mathbf{r}_1, \mathbf{r}_2, \mathbf{r}_1, \mathbf{r}_2)|\mathbf{r}_1 - \mathbf{r}_2|^2 \mathrm{d}\mathbf{r}_1 \mathrm{d}\mathbf{r}_2 / \int \rho_2(\mathbf{r}_1, \mathbf{r}_2, \mathbf{r}_1, \mathbf{r}_2)\mathrm{d}\mathbf{r}_1 \mathrm{d}\mathbf{r}_2)^{1/2}$ [26] (see the blue line), showing that the two quantities remain comparable throughout the BEC-BCS crossover[4]. We also compare the wavenumber π/x_0 of the overlap function f to the location of the dispersion minimum $k_{\rm min} = \sqrt{2m\mu}/\hbar$: they coincide in the BCS limit but differ outside, in particular because π/x_0 does not vanish (red solid curve on Fig. 3), unlike $k_{\rm min}$ (red dashed line).

In summary, we have proposed an interferometric protocol to probe the condensate wavefunction of a superfluid Fermi gas. By measuring the ↑-↓ correlations of recoiling atoms after a Ramsey-Bragg sequence, one records as a function of the interrogation time a damped oscillatory signal whose attenuation time, frequency, and asymptotic limit give access all at once to the size of the Cooper pairs, to their relative wave number, and to the macroscopic eigenvalue of the two-body density matrix. Those prominent features of fermionic condensates are difficult to access experimentally [27]. Furthermore, this method has the advantage that fine spatial resolution on ρ_2 is obtained through temporal resolution, which is rather easy to achieve. The correlation signal recorded at the end of the sequence also involves a macroscopic fraction of the atoms initially present in the trap, which makes it more robust to experimental noise. In the future, it would be interesting to extend this calculation to the case of fermions with three internal states [28].

$3N_0/8$. This disagreement with Eq. (15) is due to artifacts in the calculation of fluctuations within BCS theory, where total particle numbers are not conserved, $\langle \hat{N}_\uparrow \hat{N}_\downarrow \rangle - N_\uparrow N_\downarrow = N_0 \neq 0$ [25]. However, we expect the qualitative behavior of $S(x)$ shown in Fig. 2 to be correct as long as ρ_2 is dominated by the contribution of the condensate wavefunction ϕ_0.

---

[4] We derived the analytic expression:

$$\xi_{\rm pair}^2 = \frac{\hbar^2}{2m\Delta} \frac{4\alpha^2(\alpha + r_\alpha) + 7\alpha + 5r_\alpha}{8r_\alpha(\alpha + r_\alpha)},$$

where $\alpha = \mu/\Delta$ and $r_\alpha = \sqrt{1 + \alpha^2}$.

[1] A. L. Fetter and J. D. Walecka, *Quantum theory of many-particle systems* (McGraw-Hill, San Francisco, 1971).

[2] J.-P. Blaizot and G. Ripka, *Quantum Theory of Finite Systems* (MIT Press, Cambridge, Massachusetts, 1985).

[3] A. J. Leggett, *Quantum Liquids* (Oxford University Press, Oxford, 2006).

[4] L. Pitaevskii and S. Stringari, *Bose-Einstein Condensation and Superfluidity* (Oxford University, 2016).

[5] M. H. Anderson, J. R. Ensher, M. R. Matthews, C. E. Wieman, and E. A. Cornell, Science **269**, 198 (1995), http://www.sciencemag.org/content/269/5221/198.full.pdf.

[6] M. Greiner, C. A. Regal, and D. S. Jin, Nature **426**, 537 (2003).

[7] M. Houbiers, R. Ferwerda, H. T. C. Stoof, W. I. McAlexander, C. A. Sackett, and R. G. Hulet, Phys. Rev. A **56**, 4864 (1997).

[8] W. Zwerger, ed., *The BCS-BEC Crossover and the Unitary Fermi Gas* (Springer, Berlin, 2012).

[9] R. G. Scott, F. Dalfovo, L. P. Pitaevskii, and S. Stringari, Phys. Rev. A **86**, 053604 (2012).

[10] A. Behrle, T. Harrison, J. Kombe, K. Gao, M. Link, J. S. Bernier, C. Kollath, and M. Köhl, Nature Physics (2018), 10.1038/s41567-018-0128-6.

[11] T. Paintner, D. K. Hoffmann, M. Jäger, W. Limmer, W. Schoch, B. Deissler, M. Pini, P. Pieri, G. Calvanese Strinati, C. Chin, and J. Hecker Denschlag, Phys. Rev. A **99**, 053617 (2019).

[12] P. Dyke, A. Hogan, I. Herrera, C. C. N. Kuhn, S. Hoinka, and C. J. Vale, Phys. Rev. Lett. **127**, 100405 (2021).

[13] W. Ketterle and M. W. Zwierlein, Riv. Nuovo Cim. **31**, 247 (2008).

[14] E. Altman, E. Demler, and M. D. Lukin, Phys. Rev. A **70**, 013603 (2004).

[15] A. Polkovnikov, E. Altman, and E. Demler, Proc. Natl. Acad. Sci. U.S.A. **103**, 6125 (2006).

[16] M. Holten, L. Bayha, K. Subramanian, S. Brandstetter, C. Heintze, P. Lunt, P. M. Preiss, and S. Jochim, Nature **606**, 287 (2022).

[17] M. R. Andrews, C. G. Townsend, H.-J. Miesner, D. S. Durfee, D. M. Kurn, and W. Ketterle, Science **275**, 637 (1997), https://www.science.org/doi/abs/10.1126/science.275.5300.637.

[18] E. W. Hagley, L. Deng, M. Kozuma, M. Trippenbach, Y. B. Band, M. Edwards, M. Doery, P. S. Julienne, K. Helmerson, S. L. Rolston, and W. D. Phillips, Phys. Rev. Lett. **83**, 3112 (1999).

[19] N. Navon, A. L. Gaunt, R. P. Smith, and Z. Hadzibabic, Science **347**, 167 (2015).

[20] J. Beugnon and N. Navon, Journal of Physics B: Atomic, Molecular and Optical Physics **50**, 022002 (2017).

[21] I. Carusotto and Y. Castin, Phys. Rev. Lett. **94**, 223202 (2005).

[22] N. Navon, R. P. Smith, and Z. Hadzibabic, Nature Physics **17**, 1334 (2021).

[23] G. Veeravalli, E. Kuhnle, P. Dyke, and C. J. Vale, Phys. Rev. Lett. **101**, 250403 (2008).

[24] P. Wang, Z. Fu, L. Huang, and J. Zhang, Phys. Rev. A **85**, 053626 (2012).

[25] H. Kurkjian, Y. Castin, and A. Sinatra, Phys. Rev. A **88**, 063623 (2013).

[26] M. Marini, F. Pistolesi, and G. C. Strinati, Eur. Phys. J. B **1**, 151 (1998).

[27] C. H. Schunck, Y.-i. Shin, A. Schirotzek, and W. Ketterle, Nature **454**, 739 (2008).

[28] G. L. Schumacher, J. T. Mäkinen, Y. Ji, G. G. T. Assumpção, J. Chen, S. Huang, F. J. Vivanco, and N. Navon, arXiv (2023), 10.48550/arXiv.2301.02237, 2301.02237.